

The origin of High-velocity stars considering the impact of the Large Magellanic Cloud

JIWEI LIAO,¹ CUIHUA DU,¹ MINGJI DENG,¹ DASHUANG YE,¹ HEFAN LI,² YANG HUANG,^{1,2}
JIANRONG SHI,^{2,1} AND JUN MA^{2,1}

¹*School of Astronomy and Space Sciences, University of Chinese Academy of Sciences, Beijing 100049, P.R. China*

²*Key Laboratory of Optical Astronomy, National Astronomical Observatories, Chinese Academy of Sciences, Beijing 100012, P.R. China*

ABSTRACT

Utilizing astrometric parameters sourced from *Gaia* Data Release 3 and radial velocities obtained from various spectroscopic surveys, we identify 519 high-velocity stars (HiVels) with a total velocity in the Galactocentric restframe greater than 70% of their local escape velocity under the `Gala MilkyWayPotential`. Our analysis reveals that the majority of these HiVels are metal-poor late-type giants, and we show 9 HiVels that are unbound candidates to the Galaxy with escape probabilities of 50%. To investigate the origins of these HiVels, we classify them into four categories and consider the impact of the Large Magellanic Cloud (LMC) potential on their backward-integration trajectories. Specifically, we find that one of the HiVels can track back to the Galactic Center, and three HiVels may originate from the Sagittarius dwarf spheroidal galaxy (Sgr dSph). Furthermore, some HiVels appear to be ejected from the Galactic disk, while others formed within the Milky Way or have an extragalactic origin. Given that the LMC has a significant impact on the orbits of Sgr dSph, we examine the reported HiVels that originate from the Sgr dSph, with a few of them passing within the half-light radius of the Sgr dSph.

Keywords: High-velocity stars(736) — Stellar kinematics(1608) — Stellar dynamics(1596) — Sagittarius dwarf spheroidal galaxy(1423) — Large Magellanic Cloud(903)

1. INTRODUCTION

The existence of high-velocity stars (HiVels) implies the presence of extreme dynamics. In the literature, these stars are typically divided into four categories: hypervelocity stars (HVSs), hyper-runaway stars (HRSs), runaway stars (RSs), and high velocity halo stars (Li et al. 2021; Quispe-Huaynasi et al. 2022). The first two types of HiVels are unbound stars, with speeds exceeding the escape velocity of the Milky Way (MW). The classic origin of HVSs, as theorized by Hills (1988), involves a close encounter between a stellar binary and a massive black hole (MBH). A star that is ejected by a MBH and has an unbound velocity is defined as an HVS by Brown (2015). The

Southern Stellar Stream Spectroscopic Survey (S⁵) discovered the fastest HVS (Koposov et al. 2020), which is an A-type star with a total velocity of 1755 km s^{-1} . This star was ejected by the MBH at the Galactic Center, providing strong evidence for the Hills mechanism. HRSs are another type of unbound HiVels and are also considered as RSs with extreme velocities. One of the most plausible mechanisms for generating HRSs is the thermonuclear explosion in double white dwarf binaries (Shen et al. 2018). The first confirmed HRS is HD 271791 originating from the outer disk (Heber et al. 2008), with a total velocity of 630 km s^{-1} .

The last two types of HiVels are stars that are bound by the Galactic potential. RSs were initially introduced as O- and B-type stars with high velocities (Blaauw 1961). It is believed that RSs form in the disk and then are ejected into the halo. There are generally two main mechanisms for the formation of RSs: supernova explosions in stellar binary systems (e.g., Blaauw 1961; Portegies Zwart 2000; Wang & Han 2009; Wang et al. 2013) and dynamical encounters resulting from multi-body interactions in dense stellar systems (e.g., Bromley et al. 2009; Gvaramadze et al. 2009). High-velocity halo stars are another type of bound HiVels that could be an in-situ population of stars formed within the MW (Di Matteo et al. 2019; Belokurov et al. 2020) or an extragalactic source. Numerical simulations by Abadi et al. (2009) have shown that disrupted dwarf galaxies may contribute halo stars with high velocities. In addition to the mechanisms mentioned above, the dense environments in the cores of globular clusters facilitate many strong dynamical encounters among stellar objects (Cabrerera & Rodriguez 2023). HiVels could also be ejected through the close interaction of a globular cluster and a supermassive black hole (Capuzzo-Dolcetta & Fragione 2015), or through the formation of three-body binaries in globular clusters (Weatherford et al. 2023).

Recently, a significant number of candidate HiVels originating from the Sagittarius dwarf spheroidal galaxy (Sgr dSph) have been identified. The first candidate HVS (J1443+1453) that likely originated from the Sgr dSph was discovered by Huang et al. (2021). Subsequently, Li et al. (2022) reported 60 candidate HiVels (including 2 HVS candidates) that may also come from the Sgr dSph, and Li et al. (2023) found 15 extreme velocity stars that have had close encounters with the Sgr dSph. However, both Huang et al. (2021) and Li et al. (2023) did not consider the impact of the Large Magellanic Cloud (LMC), and Li et al. (2022) disregarded the dynamical friction from the Milky Way (MW) on the LMC. It is important to mention that the HVS3 (or HE 0437-5439) has a 40% probability of passing within 5 kpc of the LMC, taking into account the LMC's influence (Edelmann et al. 2005; Erkal et al. 2019b). It is fortunate that the *Gaia* Data Release 3 (*Gaia* DR3) provides precise proper motion measurements for HVS3. Consequently, it is necessary to investigate the origin of these HiVels.

The aim of the work is to search for more HiVels, and determine their origins considering the impact of the LMC. This paper is organized as follows: Section 2 provides a description of the observation sample. In section 3, we obtain 519 HiVels with a total velocity in the Galactocentric restframe greater than 70% of the local escape velocity. Section 4 focuses on the analysis of the origin of these HiVels. Finally, a summary is provided in Section 5.

2. OBSERVATION SAMPLE

The *Gaia* DR3 provides astrophysical parameters for 470 million stars (Gaia Collaboration et al. 2023), 34 million radial velocities (RVs) (Katz et al. 2023). To select stars with accurately measured parallax, proper motion and spectroscopic data, we applied the following criteria: $\text{RUWE} < 1.4$, $\varpi - \varpi_{\text{ZP}} > 0$, $\varpi - \varpi_{\text{ZP}} > 5\sigma_{\varpi}$ and $\text{S/N} > 10$. RUWE is Renormalized Unit Weight Error to assess the

goodness-of-fit of the astrometric solution for a particular star (Lindgren et al. 2021b). We use the approach described in Lindgren et al. (2021a) to correct *Gaia* DR3 parallaxes by the parallax zero point ϖ_{ZP} . To obtain precise RVs, we cross-matched the *Gaia* DR3 catalog with other large-scale Galactic Surveys, such as GALAH DR3 (De Silva et al. 2015; Buder et al. 2021), LAMOST DR10 (Cui et al. 2012; Zhao et al. 2012), RAVE DR6 (Steinmetz et al. 2020), APOGEE DR17 (Majewski et al. 2017), and S⁵ (Li et al. 2019)). The weighted mean RV was computed using the following equation:

$$rv = \frac{\sum_i^N w_i rv_i}{\sum_i^N w_i}, \quad (1)$$

where rv represents the calculated radial velocity, $w_i = 1/\sigma_i^2$ is the weight corresponding to each measurement with uncertainty σ_i , and N is the total number of measurements. We removed stars for which $|rv - rv_{\text{Gaia}}| \geq 3\sigma_{\text{Gaia}}$. In the context of this analysis, rv , rv_{Gaia} , and rv_{Survey} correspond to the corrected radial velocity, the radial velocity from *Gaia*, and the radial velocity from other surveys, respectively. Figure 1 demonstrates that the difference in radial velocities among the 519 HiVels is minimal, with a majority falling within 15 km s^{-1} . Using the *Gaia*'s parameters such as `phot_variable_flag`, and `classprob_dsc_combmod_star` flag which represents the probability of being a single star (but not a white dwarf) from DSC-Combmod (which classifies objects using BP/RP spectrum, photometry and astrometry features), we removed all variable stars and the 519 HiVels are single stars.

Adopting the same method as Du et al. (2019), we use Bayesian analysis to determine heliocentric distances (d) and velocities in the R.A. and Decl. direction (ν_α and ν_δ). The posterior consists of likelihood with a three-dimensional Gaussian distribution and prior with the three-parameter generalized Gamma distribution (Bailer-Jones et al. 2021):

$$P(\theta|\chi) \propto e^{-\frac{1}{2}(\chi-m(\theta))^T C_\chi^{-1}(\chi-m(\theta))} \frac{1}{\Gamma(\frac{\beta+1}{\alpha})} \frac{\alpha}{L^{\beta+1}} r^\beta e^{-(\frac{r}{L})^\alpha}, \quad (2)$$

where $\theta = [d, \nu_\alpha, \nu_\delta]$, $\chi = [\varpi, \mu_{\alpha*}, \mu_\delta]$, $m = [1/d + \varpi_{\text{ZP}}, \nu_\alpha/kd, \nu_\delta/kd]$, $k = 4.74047$, and C_χ is covariance matrix.

We implement the Markov Chain Monte Carlo (MCMC) sampler `emcee` (Foreman-Mackey et al. 2013) to draw samples from the posterior probability, and generate 4000 Monte Carlo (MC) realizations for each object (stars, dwarf galaxies, and globular clusters). Following the approach outlined in Liao et al. (2023), we adopt the position of the Sun to the Galactic Centre $(x_\odot, y_\odot, z_\odot) = (8.122, 0, 0.0208) \text{ kpc}$ (GRAVITY Collaboration et al. 2018; Bennett & Bovy 2019) and solar velocity of $(U_\odot, V_\odot, W_\odot) = (11.1, 245, 7.25) \text{ km s}^{-1}$ (Schönrich et al. 2010; McMillan 2017) to derive 3D velocities (U, V, W) (Johnson & Soderblom 1987) and position of each star in the Cartesian Galactocentric coordinate system (Jurić et al. 2008).

3. HIVELS SAMPLE

In order to determine the origin of the HiVels, we rewind them in the combined presence of the gravitational field of the MW and LMC. For the MW, we adopt the `Gala` potential `MilkyWayPotential` (Price-Whelan 2017), including the Hernquist (Hernquist 1990) bulge and nucleus, the Miyamoto-Nagai (Miyamoto & Nagai 1975) stellar disk, and the Navarro-Frenk-White (Navarro et al. 1996) dark matter halo. For the LMC, we consider a Plummer profile with a mass of $1.38 \times 10^{11} M_\odot$ (Erkal

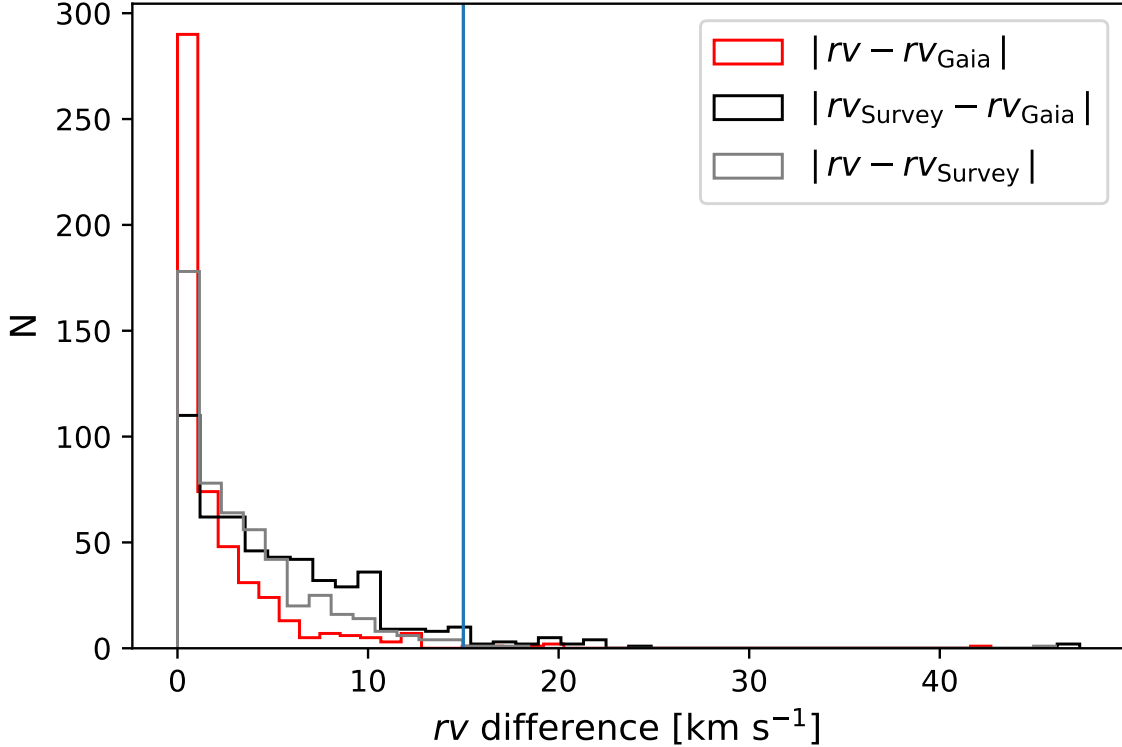


Figure 1. Distribution of radial velocity differences ($|rv - rv_{\text{Gaia}}|$, $|rv_{\text{Survey}} - rv_{\text{Gaia}}|$, $|rv - rv_{\text{Survey}}|$) for the 519 HiVels. The corrected radial velocities, the radial velocities from Gaia, and the radial velocities from other surveys are represented by rv , rv_{Gaia} , and rv_{Survey} , respectively. For reference, a vertical blue line is plotted at a difference of 15 km s^{-1} .

et al. 2019a) and dynamical friction from the MW on the LMC taking the prescription from Petts et al. (2016). We have set the half-mass radius to 5 kpc for definiteness. The scale radius is set at 17 kpc, computed based on an enclosed mass of $1.7 \times 10^{10} M_{\odot}$ within 8.7 kpc (van der Marel & Kallivayalil 2014). The analysis is conducted with the LMC’s position, radial velocity and proper motions from Erkal et al. (2019b). The dynamical friction and LMC’s gravitational potential use the ChandrasekharDynamicalFrictionForce function and MovingObjectPotential function implemented in galpy (Bovy 2015), respectively. We then integrate the backward orbit **using** galpy over a total time of 3 Gyr with a time step of 0.1 Myr .

If a star is ejected from the Galactic disk, its backward-integral trajectory passes through the Galactic midplane ($Z_{\text{GC}} = 0 \text{ kpc}$ plane) with a maximum distance of 25 kpc from the node to the Galactic Center (Marchetti 2021). In addition, a HiVel tracking back to the Galactic Center should intersect the Galactic midplane only once, and its backward-integral trajectory pass within 1 kpc of the Galactic Center (Liao et al. 2023). For HiVels originating from the Sgr dSph, their backward-integral trajectories are expected to pass within the Sgr dSph’s half-light radius of 2.587 kpc (McConnachie 2012). In the case of a HiVel originating from a globular cluster, it needs to pass within the Plummer scale radius of that cluster (Vasiliev & Baumgardt 2021). The probabilities were calculated by tallying the frequency of occurrence in the 4000 MC realizations conducted in this study.

The HiVels sample is defined as stars with total velocities (ν_{GC}) in the Galactocentric restframe exceeding 70% of the escape velocity ($\nu_{\text{GC}} > 0.7 \nu_{\text{esc}}$). From this definition, a final sample of 519 HiVels

with astrometric parameters and radial velocities was derived, including 9 unbound **candidates** ($P_{\text{ub}} > 0.5$). The density distribution of these stars in ν_{GC} and r_{GC} is shown in Figure 2. The number of HiVels is the highest at a distance of 8.1 kpc and gradually decreases on both sides. This aligns with the observed number of stars. As the Sun is positioned at a distance of 8.12 kpc (GRAVITY Collaboration et al. 2018), the count of observed stars gradually diminishes towards the outer regions. We also plot the Hertzsprung–Russell diagram of these stars’ astrophysical parameters (T_{eff} , $\log g$, $[\text{Fe}/\text{H}]$) in Figure 3. Most of them are the metal-poor late-type giants with $[\text{Fe}/\text{H}] < -0.8$ dex and $T_{\text{eff}} < 7300$ K.

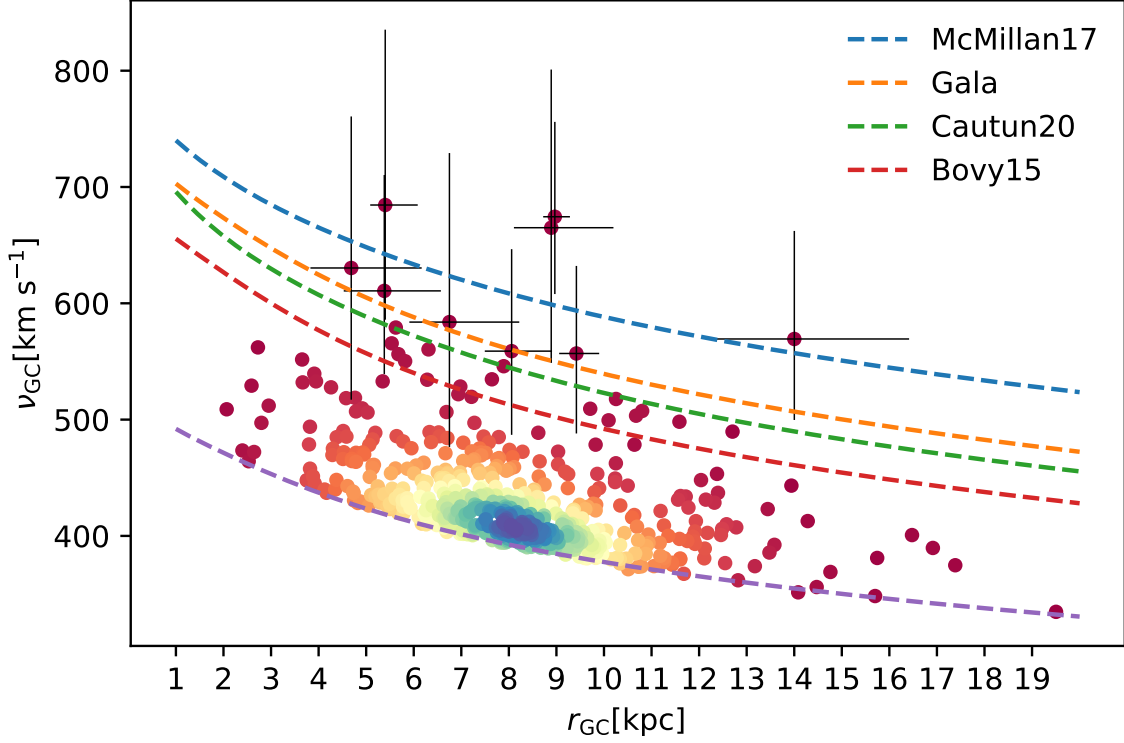


Figure 2. The density distribution of total velocity ν_{GC} vs. Galactocentric distance r_{GC} for the final sample 519 HiVels with $\nu_{\text{GC}} > 0.7\nu_{\text{esc}}$, including 9 unbound candidates ($P_{\text{ub}} > 0.5$) with error bars under the Gala (Price-Whelan 2017) MilkyWayPotential. The four different colored dashed lines are the escape velocity curves derived from the four different Milky Way potential models (McMillan 2017; Price-Whelan 2017; Cautun et al. 2020; Bovy 2015), respectively. The purple dashed line represents 70% of the escape velocity curve from the Gala.

4. THE ORIGIN OF HIVELS

4.1. Classification of HiVels

Table 1 gives the classification criteria of HiVels. Detailed information about 9 unbound stars (8 for the first time, and 2 reported by Marchetti (2021) and Li et al. (2021)) is provided in Table 2. Two of these stars exhibit retrograde motion relative to the direction of the MW’s rotation ($\nu_{\phi} < 0$), and their trajectories do not track back to the Galactic disk ($P_{\text{disk}} < 0.5$), suggesting a possible extragalactic origin. Furthermore, 57 bound HiVels ($P_{\text{ub}} < 0.5$) exhibit prograde motion and cluster

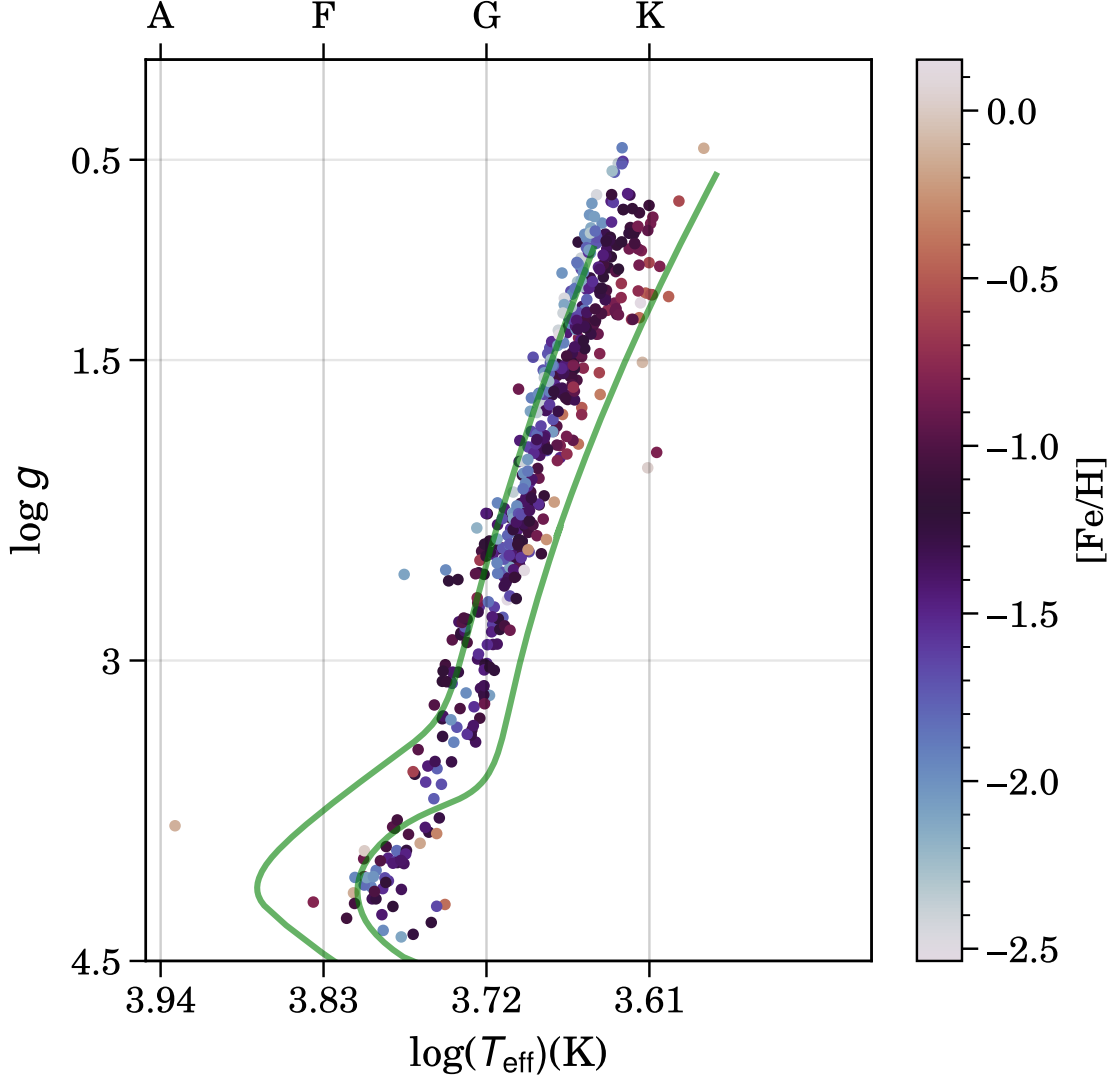


Figure 3. A total of **513** HiVels from the final sample are shown in the $\log g$ vs. T_{eff} diagram, and the color is coded by metallicity. The right and left green lines represent MIST isochrones (Dotter 2016; Choi et al. 2016; Paxton et al. 2011, 2013, 2015) with $[M/H] = -0.5$, $\log(\text{Age}) [\text{year}] = 9.8$ (100 Myr), and $[M/H] = -2$, $\log(\text{Age}) [\text{year}] = 9.8$ (100 Myr), respectively.

at high metallicity, and their trajectories track back to the galactic disk ($P_{\text{disk}} > 0.5$), indicating they are likely the runaway stars (RSs) that form in the disk and then are ejected into the halo but not the typical OB type runaway stars. The remaining 453 HiVels are classified as high-velocity halo stars that may form within the MW or have extragalactic origins.

4.2. A HiVel track back to the Galactic Center

Table 1. The classification criteria of HiVels

Class	P_{ub}	P_{disk}	ν_{ϕ}	MBH ejection origin
Hypervelocity star (HVS)	> 0.5	True
Hyper-runaway star (HRS)	> 0.5	> 0.5	$> -276.7 \times [\text{Fe}/\text{H}] - 97.78$	False
Runaway star (RS)	< 0.5	> 0.5	$> -276.7 \times [\text{Fe}/\text{H}] - 97.78$	False
High velocity halo star	< 0.5

NOTE—The formula $\nu_{\phi} = -276.7 \times [\text{Fe}/\text{H}] - 97.78$, proposed by Li et al. (2023), serves as an empirical demarcation line for distinguishing between the disk stars and the halo stars. P_{ub} and P_{disk} represent the probability of exceeding the Galactic escape velocity curves and the probability of tracking back to the Galactic disk, respectively.

Table 2. Basic parameters for the 9 unbound candidates

Gaia DR3 source_id	R.A. (deg)	Decl. (deg)	rv (km s^{-1})	d (kpc)	ν_{GC} (km s^{-1})	P_{ub}	P_{disk}	ν_{ϕ} (km s^{-1})
1309092223502856576	257.4199	29.9771	-487 ± 1	$16.12^{+3.00}_{-2.24}$	570^{+92}_{-70}	0.729	0.002	145^{+142}_{-112}
1204061267883975040	238.1112	20.1969	-263 ± 1	$10.36^{+1.77}_{-1.36}$	652^{+149}_{-103}	0.825	0.007	-186^{+185}_{-77}
1297316350890352000	248.1776	21.2721	-335 ± 1	$9.60^{+1.33}_{-1.05}$	559^{+88}_{-72}	0.505	0.045	-26^{+75}_{-80}
4263403134667526144	292.1825	-0.0883	-25 ± 2	$8.44^{+1.48}_{-1.04}$	694^{+142}_{-108}	0.793	1	276^{+176}_{-114}
6098873935647575552	220.6411	-44.5675	163 ± 1	$10.72^{+1.98}_{-1.43}$	582^{+147}_{-106}	0.530	0.999	345^{+200}_{-145}
6241679678390298880	236.9944	-20.5118	-305 ± 1	$10.90^{+1.61}_{-1.31}$	616^{+171}_{-103}	0.549	0.043	574^{+102}_{-144}
6235773131986833792	239.3821	-24.9635	-156 ± 1	$10.78^{+1.92}_{-1.55}$	620^{+140}_{-103}	0.549	0.972	592^{+163}_{-210}
1383279090527227264	240.3373	41.1668	-185 ± 1	$6.59^{+0.61}_{-0.52}$	676^{+80}_{-68}	0.967	1	-487^{+39}_{-37}
1375165725506487424	231.8486	36.0344	-86 ± 1	$7.79^{+0.83}_{-0.70}$	553^{+79}_{-65}	0.546	1	-319^{+21}_{-26}

NOTE—The last two rows list the stars that have been reported by Marchetti (2021); Li et al. (2021).

We found a HiVel that crosses over the Galactic midplane ($Z_{\text{GC}} = 0$ kpc plane) only once and has a backwards-integrated trajectory passing within 1 kpc of the Galactic Center. Table 3 shows the detailed information. Since the Galactic field is a classically collisionless system, particularly at the high speeds typical of HiVels, we neglect the perturbative influence of other bodies on these orbits. According to the Hills mechanism ejection probability proposed by Bromley et al. (2006), the HiVel is not close enough to the Galactic Center, making it unlikely to be ejected by this mechanism. We computed the trajectories of 150 globular clusters from Vasiliev (2019) using proper motions from Vasiliev & Baumgardt (2021), but this star does not pass within their Plummer scale radius. Interestingly, the star is similar in metallicity and age to the VVV CL002 ($[\text{Fe}/\text{H}] = -0.4 \pm 0.2$, age > 6.5 Gyr) (Moni Bidin et al. 2011), which is the closest globular cluster to the Galactic Center

Table 3. Detailed information about the star with probable origin in the center of the Galaxy.

Parameter	value	unit
<i>Gaia</i> DR3 source_id	6236463526512162944	
GALAH DR3 subject_id	170603004101340	
rv	-144 ± 0.3	km s^{-1}
d	$7.04^{+1.05}_{-0.84}$	kpc
ν_{GC}	552^{+89}_{-68}	km s^{-1}
P_{cross}	0.761	
r_{closest}	$0.79^{+0.84}_{-0.34}$	kpc
[Fe/H]	-0.58 ± 0.09	dex
T_{eff}	3891 ± 93	K
log g	0.71 ± 0.54	dex
Age	6.8767	Gyr
Mass	1.07	M_{\odot}

NOTE— P_{cross} and r_{closest} are the probability of crossing over the Galactic midplane only once and the distance of the backward-integral trajectory closest to the Galactic center, respectively. The last five rows of data come from GALAH DR3.

(Minniti et al. 2021). However, due to the lack of radial velocity information for this globular cluster, it is unknown whether the star passed within its Plummer scale radius.

4.3. *HiVels* originated from the Sgr dSph and the LMC

In our sample of *HiVels*, three *HiVels* (2 for the first time, and 1 reported by Li et al. (2022); Li et al. (2023)) show potential origin from the Sgr dSph. Their backward-integrated trajectories can track back to the Sgr dSph ($P_{\text{Sgr}} > 0.5$) and other parameters are listed in Table 5. The chemical abundance ([Fe/H] = -1.12 ± 0.02 , $[\alpha/\text{Fe}] = 0.27 \pm 0.01$) of *Gaia* DR3 3702750168409332864 is consistent with the members stars of the Sgr stream which are taken from an analysis based on the LAMOST K giants (Huang et al. 2021; Yang et al. 2019). The color-magnitude (BP-RP = 0.96, $M_{\text{G}} = 0.21$) of *Gaia* DR3 3653273996289384832 is most similar to both the Sgr and Sgr stream (e.g., Li et al. 2022; Vasiliev & Belokurov 2020; Vasiliev et al. 2021)

It is evident that the LMC significantly influences the orbit of the Sgr dSph as shown in Figure 4. As the *HiVels* that reported to originate from the Sgr dSph (Li et al. 2022; Huang et al. 2021; Li et al. 2023) did not consider the impact or the dynamical friction from the MW on the LMC, we recalculated the probabilities P_{Sgr} of their trajectories passing within the half-light radius of the Sgr dSph. Among them, the *HiVels* with $P_{\text{Sgr}} > 0.5$ are listed in Table 5. We also calculated the

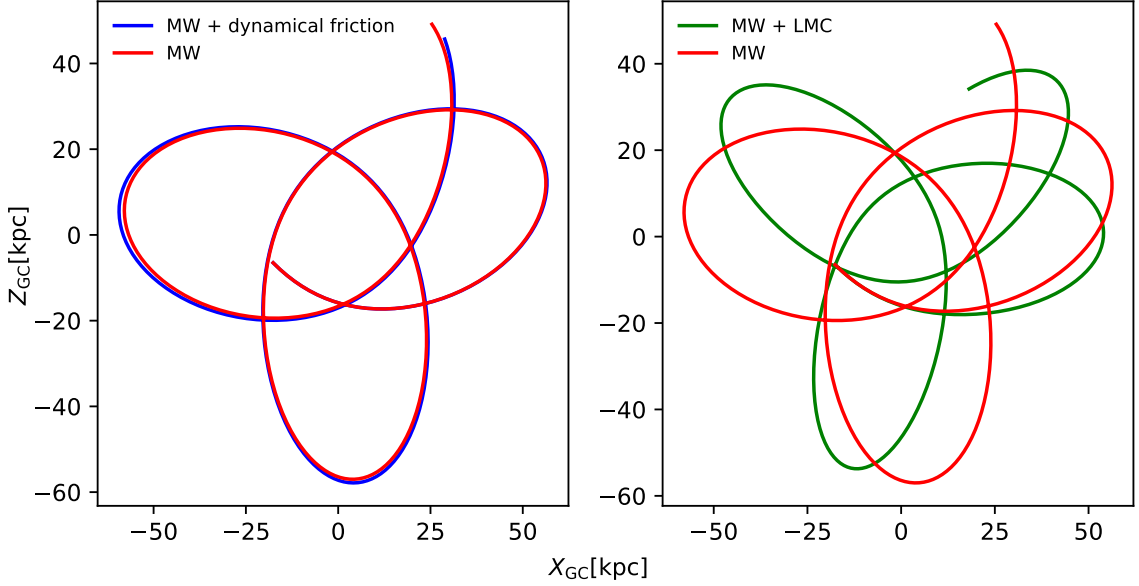


Figure 4. The left panel illustrates the orbits without dynamical friction from the MW on the Sgr dSph and with dynamical friction, showing minimal differences. In contrast, the right panel shows the orbits without and with the potential of the LMC, displaying significant differences in the orbits caused by the LMC’s gravitational potential.

Table 4. The related parameters of HVS3

Parameter	value	unit
R.A.	04 : 38 : 12.8	
Decl.	−54 : 33 : 12	
rv	723 ± 3	km s^{-1}
d	61 ± 10	kpc
μ_{α^*}	0.853 ± 0.049	mas yr^{-1}
μ_{δ}	1.614 ± 0.061	mas yr^{-1}
$\text{Corr}(\mu_{\alpha^*}, \mu_{\delta})$	−0.086	

NOTE—The first four rows refer to Erkal et al. (2019b), and the last three rows are from *Gaia* DR3.

trajectory of HVS3 (Erkal et al. 2019b) using the proper motion provided by *Gaia* DR3, and related parameters are listed in Table 4. HVS3 has a 37% probability passing within 5 kpc of the LMC, and we show contours of the time of closest approach to the LMC and the velocity during this closest approach in Figure 5.

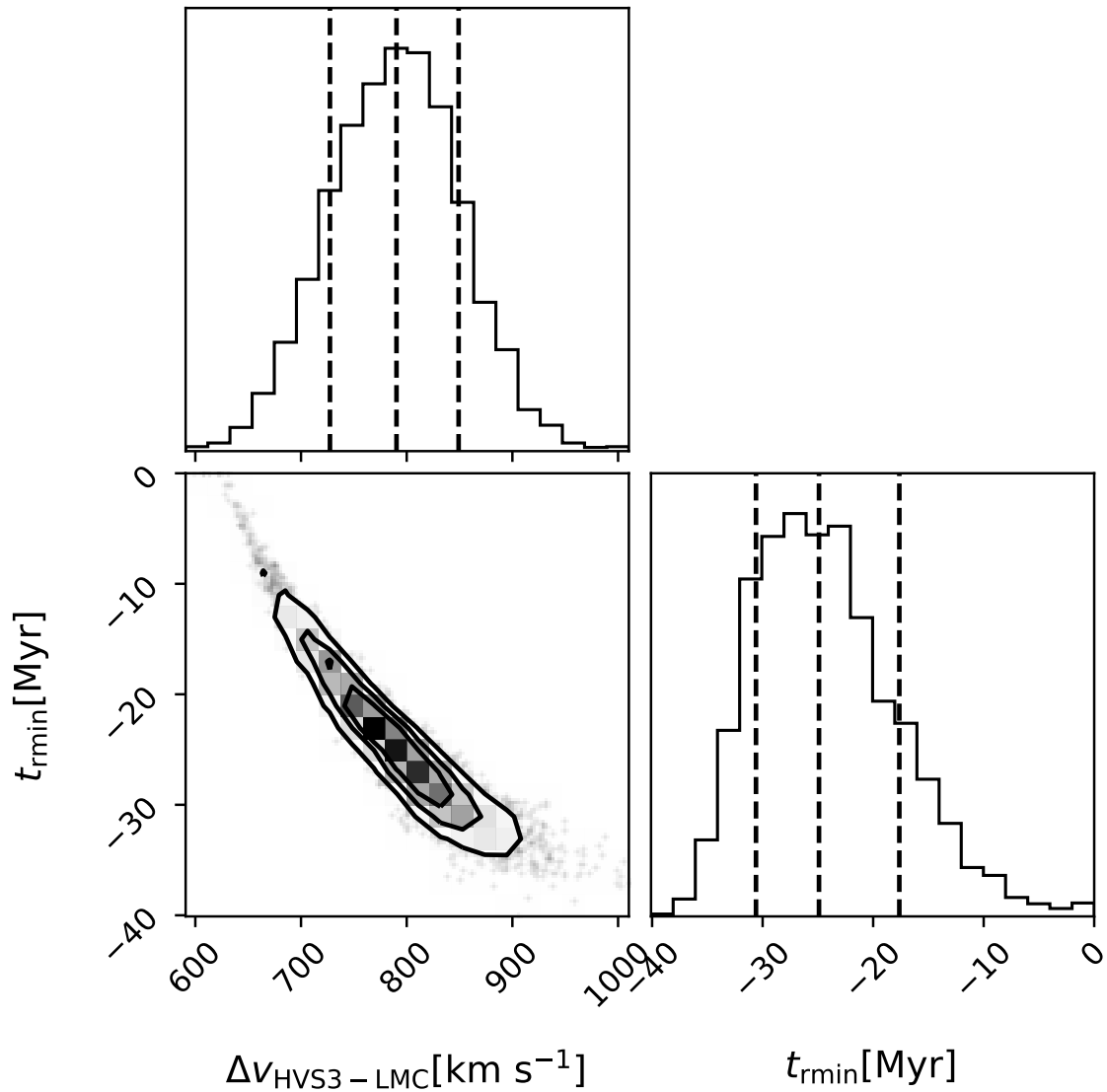


Figure 5. Distribution of the velocity and time at closest approach to LMC. The dashed lines show the 16,50,84 percentiles of 1D distribution. The velocity is 790^{+59}_{-63} km s $^{-1}$. The backward time is $24.9^{+5.7}_{-7.3}$ Myr.

Table 5. HiVels originating from the Sgr dsph

Gaia DR3 source_id	rv (km s ⁻¹)	d (kpc)	ν_{GC} (km s ⁻¹)	P_{Sgr} ...	G -magnitude ^a mag	BP-RP ^a mag	[Fe/H] dex	[α /Fe] dex	Reference
3702750168409332864	465 ± 3	2.47 ^{+0.15} _{-0.13}	410 ⁺³ ₋₂	0.64	14.4	0.96	-1.23 ± 0.02 ^b	0.27 ± 0.01 ^b	(1)
3653273996289384832	337 ± 4	5.39 ^{+0.62} _{-0.51}	505 ⁺³⁹ ₋₂₈	0.96	13.9	0.96	-1.02 ± 0.09 ^b	...	(1)
3793871060689209984	507 ± 1	2.30 ^{+0.12} _{-0.10}	419 ⁺¹ ₋₁	1.0	11.3	1.18	-1.02 ± 0.28 ^c	...	(1)(2)(3)
564961308084113152	-70 ± 3	2.40 ^{+0.06} _{-0.06}	417 ⁺¹² ₋₁₂	1.0	12.3	1.18	(2)
1805174788871484800	-368 ± 3	3.80 ^{+0.23} _{-0.20}	415 ⁺¹⁷ ₋₁₄	0.92	12.6	0.89	(2)
4423441557511145088	226 ± 2	8.02 ^{+1.18} _{-0.96}	422 ⁺⁵² ₋₃₈	0.60	12.8	1.54	(2)
6716076404123420288	-278 ± 4	3.06 ^{+0.14} _{-0.13}	488 ⁺¹⁵ ₋₁₅	0.93	12.3	1.29	(2)
6734684023516484096	-334 ± 0	8.50 ^{+1.11} _{-0.88}	501 ⁺⁴⁵ ₋₃₃	0.58	13.1	1.50	-1.21 ± 0.01	0.22 ± 0.01	(2)
383206057417413248	-313 ± 13	1.48 ± 0.07	443 ± 19	1.0	15.3	0.76	(3)
1282270187101294592	184 ± 13	2.53 ± 0.34	439 ± 55	0.57	16.69	0.72	(3)
1962742265496273920	-318 ± 3	1.72 ± 0.27	452 ± 66	0.62	17.55	1.31	(3)

NOTE—Reference: (1) this work; (2) Li et al. (2022); (3) Li et al. (2023). [^a]: G -magnitude and BP-RP from *Gaia* DR3. [^b]: Data from LAMOST DR10. [^c]: Data from RAVE DR6.

5. SUMMARY AND DISCUSSION

In this study, we identify a total of 519 high-velocity stars (HiVels) through a cross-matching process between the *Gaia* DR3 and other Large-scale Galactic Surveys. A catalog of the properties of these stars is available on China-VO: [doi:10.12149/101304](https://doi.org/10.12149/101304). These HiVels consist of 9 unbound candidates under the *Gala MilkyWayPotential*, 57 runaway stars (not the typical OB type runaway stars), and 453 high-velocity halo stars. In our sample, 78 HiVels have been reported by [Li et al. \(2021\)](#), a candidate HiVel originating from the Sgr dSph has been reported by [Li et al. \(2022\)](#), and 440 have been reported for the first time.

The *Gaia* *G*-band magnitudes of these HiVels are less than 15 and majority of these stars are metal-poor late-type giants. Although we employ geometric distances rather than photogeometric or photo-astrometric distances, they are very similar at $G < 15$ as shown in [Anders et al. \(2022\)](#). The backwards-integrated trajectory of a HiVel can track back to the Galactic Center but there is insufficient evidence for the VVV CL002 origin. Notably, based on the color-magnitude or chemical analysis, as well as the trajectories, three HiVels could be the member stars of the Sgr dSph. If the LMC has not been taken into account in the orbital analysis, we still obtain the same results for the four stars, as they are far from the LMC (over 50 kpc) and have a short time to their pericenter (57 Myr ago). Considering the impact of the LMC, only a small number of reported HiVels pass within the half-light radius of the Sgr dSph. This is because the LMC has a significant impact on the orbit of the Sgr dSph and HiVels originating from the Sgr dSph are required to pass within the half-light radius of the Sgr dSph. Using the *Gaia* DR3's proper motion, HVS3 may still come from the LMC. In the near future, we anticipate the radial velocity of VVV CL002 to be observed, which will enable us to calculate its orbit to determine the origin of the HiVel tracking back to the Galactic Center. We also expect that the future surveys will provide a rich source of more HiVels to provide new insights for understanding the presence of an extreme dynamic in the Galaxy.

ACKNOWLEDGMENTS

We thank especially the referee for insightful comments and suggestions, which have improved the paper significantly. We are grateful to Jo Bovy for his helpful advice on orbital integration. This work was supported by the National Natural Science Foundation of China (NSFC Nos: 12090040, 12090044, 11973042, 11973052, and 11873053). It was also supported by the Fundamental Research Funds for the Central Universities and the National Key R&D Program of China No. 2019YFA0405501. This work has made use of data from the European Space Agency (ESA) mission *Gaia* (<https://www.cosmos.esa.int/gaia>), processed by the *Gaia* Data Processing and Analysis Consortium (DPAC, <https://www.cosmos.esa.int/web/gaia/dpac/consortium>). Funding for the DPAC has been provided by national institutions, in particular the institutions participating in the *Gaia* Multilateral Agreement.

This work has made use of data from the European Space Agency (ESA) mission *Gaia* (<https://www.cosmos.esa.int/gaia>), processed by the *Gaia* Data Processing and Analysis Consortium (DPAC, <https://www.cosmos.esa.int/web/gaia/dpac/consortium>). Funding for the DPAC has been provided by national institutions, in particular the institutions participating in the *Gaia* Multilateral Agreement.

This work made use of the Third Data Release of the GALAH Survey. This paper includes data that has been provided by AAO Data Central (datacentral.aao.gov.au). It also made use of the Sixth Data Release of the RAVE Survey. Guoshoujing Telescope (the Large Sky Area Multi-Object

Fiber Spectroscopic Telescope LAMOST) is a National Major Scientific Project built by the Chinese Academy of Sciences. Funding for the project has been provided by the National Development and Reform Commission. Funding for the Sloan Digital Sky Survey IV has been provided by the Alfred P. Sloan Foundation, the U.S. Department of Energy Office of Science, and the Participating Institutions. SDSS-IV acknowledges support and resources from the Center for High Performance Computing at the University of Utah. The SDSS website is www.sdss.org. Based on data acquired at the Anglo-Australian Telescope. We acknowledge the traditional owners of the land on which the AAT stands, the Gamilaraay people, and pay our respects to elders past and present.

APPENDIX

A. CATALOG FORMAT

Table 6 describes the format of the full table for the 519 HiVels with a total velocity in the Galactocentric restframe greater than 70% of the local escape velocity. It is available in a machine-readable format in the online Journal and in China-VO.

Table 6. Catalog Format

Label	Unit	Description
designation	—	Unique source designation, Gaia DR3
RAdeg	deg	Right ascension, decimal degrees, Gaia DR3 (ICRS at Epoch=2016.0)
DEdeg	deg	Declination, decimal degrees, Gaia DR3 (ICRS at Epoch=2016.0)
plx	mas	Parallax, Gaia DR3
e_plx	mas	Error of plx, Gaia DR3
plx-zp	mas	Parallax zero-point correction, after Lindegren et al. (2021b)
pmRA	mas.yr-1	Proper motion in right ascension direction, Gaia DR3
e_pmRA	mas.yr-1	Error of pmRA
pmDE	mas.yr-1	Proper motion in declination direction, Gaia DR3
e_pmDE	mas.yr-1	Error of pmDE
plx_pmra-corr	—	Correlation between parallax and proper motion in right ascension, Gaia DR3
plx_pmdec-corr	—	Correlation between parallax and proper motion in declination, Gaia DR3
pmra_pmdec-corr	—	Correlation between proper motion in right ascension and in declination, Gaia DR3
ruwe	—	Renormalised unit weight error, Gaia DR3
Gmag	mag	G-band mean magnitude, Gaia DR3 [phot_g_mean_mag]
bp-rp	mag	BP-RP color, Gaia DR3 [phot_bp_mean_mag - phot_rp_mean_mag]
cross-match-sur	—	Cross-match the name of survey id
surveyid	—	Unique ID in the survey [survey_id]
Teff	K	Effective temperature, the cross-match survey

Table 6 continued on next page

Table 6 (*continued*)

Label	Unit	Description
e_Teff	K	Error of Teff
logg	[cm.s-2]	Surface gravity, the cross-match survey
e_logg	[cm.s-2]	Error of logg
FeH	[-]	Metallicity, the cross-match survey
e_FeH	[-]	Error of metallicity
a_FeH	[-]	Alpha abundance, the cross-match survey
e_a_FeH	[-]	Error of a/FeH
RVel	km.s-1	Weighted mean radial velocity, Equation 1
e_RVel	km.s-1	Error of radial velocity
GGDrln	—	Corresponding to L in equation 2, after Bailer-Jones et al. (2021)
GGDalpha	—	Corresponding to α in equation 2, after Bailer-Jones et al. (2021)
GGDbeta	—	Corresponding to β in equation 2, after Bailer-Jones et al. (2021)
Dist	kpc	Heliocentric distance (after Du et al. (2019))
e_Dist	kpc	Lower uncertainty on Dist
E_Dist	kpc	Upper uncertainty on Dist
RGC	kpc	Galactocentric distance (after Du et al. (2019))
e_RGC	kpc	Lower uncertainty on RGC
E_RGC	kpc	Upper uncertainty on RGC
VGC	km.s-1	Galactocentric total velocity (after Du et al. (2019))
e_VGC	km.s-1	Lower uncertainty on VGC
E_VGC	km.s-1	Upper uncertainty on VGC
Vphi	km.s-1	Rotation velocity, this work
P-ub	—	Unbound possibility, this work
P-disk	—	Probability of the star tracking back to the disk, this work
P-sgr	—	Probability of the star tracking back to the Sgr, this work
var-flag	—	Flag indicating if variability was identified in the photometric data, Gaia DR3 [phot_variable_flag]
Pstar	—	Probability from DSC-Combmod of being a single star, Gaia DR3, [classprob_dsc_combmod_star]
RVel-DR3	km.s-1	Gaia DR3 radial velocity
e_RVel-DR3	km.s-1	Error of RVel-DR3

NOTE—Table 6 is published in its entirety in the machine-readable format. A portion is shown here for guidance regarding its form and content. It is also available on China-VO: [doi:10.12149/101304](https://doi.org/10.12149/101304)

REFERENCES

- Abadi, M. G., Navarro, J. F., & Steinmetz, M. 2009, *ApJL*, 691, L63, doi: [10.1088/0004-637X/691/2/L63](https://doi.org/10.1088/0004-637X/691/2/L63)
- Anders, F., Khalatyan, A., Queiroz, A. B. A., & Chiappini, C. 2022, *A&A*, 658, A91, doi: [10.1051/0004-6361/202142369](https://doi.org/10.1051/0004-6361/202142369)
- Bailer-Jones, C. A. L., Rybizki, J., Fouesneau, M., Demleitner, M., & Andrae, R. 2021, *AJ*, 161, 147, doi: [10.3847/1538-3881/abd806](https://doi.org/10.3847/1538-3881/abd806)
- Belokurov, V., Sanders, J. L., Fattahi, A., Smith, M. C., & Deason, A. J. 2020, *Monthly Notices of the Royal Astronomical Society*, 494, 3880, doi: [10.1093/mnras/staa876](https://doi.org/10.1093/mnras/staa876)
- Bennett, M., & Bovy, J. 2019, *MNRAS*, 482, 1417, doi: [10.1093/mnras/sty2813](https://doi.org/10.1093/mnras/sty2813)
- Blaauw, A. 1961, *BAN*, 15, 265
- Bovy, J. 2015, *ApJS*, 216, 29, doi: [10.1088/0067-0049/216/2/29](https://doi.org/10.1088/0067-0049/216/2/29)
- Bromley, B. C., Kenyon, S. J., Brown, W. R., & Geller, M. J. 2009, *ApJ*, 706, 925, doi: [10.1088/0004-637X/706/2/925](https://doi.org/10.1088/0004-637X/706/2/925)
- Bromley, B. C., Kenyon, S. J., Geller, M. J., et al. 2006, *ApJ*, 653, 1194, doi: [10.1086/508419](https://doi.org/10.1086/508419)
- Brown, W. R. 2015, *ARA&A*, 53, 15, doi: [10.1146/annurev-astro-082214-122230](https://doi.org/10.1146/annurev-astro-082214-122230)
- Buder, S., Sharma, S., Kos, J., Amarsi, A. M., & Nordlander, T. 2021, *MNRAS*, 506, 150, doi: [10.1093/mnras/stab1242](https://doi.org/10.1093/mnras/stab1242)
- Cabrera, T., & Rodriguez, C. L. 2023, arXiv e-prints, arXiv:2302.03048, doi: [10.48550/arXiv.2302.03048](https://doi.org/10.48550/arXiv.2302.03048)
- Capuzzo-Dolcetta, R., & Fragione, G. 2015, *MNRAS*, 454, 2677, doi: [10.1093/mnras/stv2123](https://doi.org/10.1093/mnras/stv2123)
- Cautun, M., Benítez-Llambay, A., Deason, A. J., Frenk, C. S., & Fattahi, A. 2020, *MNRAS*, 494, 4291, doi: [10.1093/mnras/staa1017](https://doi.org/10.1093/mnras/staa1017)
- Choi, J., Dotter, A., Conroy, C., & Cantiello, M. 2016, *ApJ*, 823, 102, doi: [10.3847/0004-637X/823/2/102](https://doi.org/10.3847/0004-637X/823/2/102)
- Cui, X.-Q., Zhao, Y.-H., Chu, Y.-Q., Li, G.-P., & Li, Q. 2012, *Research in Astronomy and Astrophysics*, 12, 1197, doi: [10.1088/1674-4527/12/9/003](https://doi.org/10.1088/1674-4527/12/9/003)
- De Silva, G. M., Freeman, K. C., Bland-Hawthorn, J., Martell, S., & de Boer, E. W. 2015, *MNRAS*, 449, 2604, doi: [10.1093/mnras/stv327](https://doi.org/10.1093/mnras/stv327)
- Di Matteo, P., Haywood, M., Lehnert, M. D., Katz, D., & Khoperskov, S. 2019, *A&A*, 632, A4, doi: [10.1051/0004-6361/201834929](https://doi.org/10.1051/0004-6361/201834929)
- Dotter, A. 2016, *ApJS*, 222, 8, doi: [10.3847/0067-0049/222/1/8](https://doi.org/10.3847/0067-0049/222/1/8)
- Du, C., Li, H., Yan, Y., Newberg, H. J., & Shi, J. 2019, *ApJS*, 244, 4, doi: [10.3847/1538-4365/ab328c](https://doi.org/10.3847/1538-4365/ab328c)
- Edelmann, H., Napiwotzki, R., Heber, U., Christlieb, N., & Reimers, D. 2005, *ApJL*, 634, L181, doi: [10.1086/498940](https://doi.org/10.1086/498940)
- Erkal, D., Belokurov, V., Laporte, C. F. P., Koposov, S. E., & Li, T. S. 2019a, *MNRAS*, 487, 2685, doi: [10.1093/mnras/stz1371](https://doi.org/10.1093/mnras/stz1371)
- Erkal, D., Boubert, D., Gualandris, A., Evans, N. W., & Antonini, F. 2019b, *MNRAS*, 483, 2007, doi: [10.1093/mnras/sty2674](https://doi.org/10.1093/mnras/sty2674)
- Foreman-Mackey, D., Hogg, D. W., Lang, D., & Goodman, J. 2013, *PASP*, 125, 306, doi: [10.1086/670067](https://doi.org/10.1086/670067)
- Gaia Collaboration, Vallenari, A., Brown, A. G. A., et al. 2023, *A&A*, 674, A1, doi: [10.1051/0004-6361/202243940](https://doi.org/10.1051/0004-6361/202243940)
- GRAVITY Collaboration, Abuter, R., Amorim, A., Anugu, N., & Bauböck, M. 2018, *A&A*, 615, L15, doi: [10.1051/0004-6361/201833718](https://doi.org/10.1051/0004-6361/201833718)
- Gvaramadze, V. V., Gualandris, A., & Portegies Zwart, S. 2009, *MNRAS*, 396, 570, doi: [10.1111/j.1365-2966.2009.14809.x](https://doi.org/10.1111/j.1365-2966.2009.14809.x)
- Heber, U., Edelmann, H., Napiwotzki, R., Altmann, M., & Scholz, R. D. 2008, *A&A*, 483, L21, doi: [10.1051/0004-6361:200809767](https://doi.org/10.1051/0004-6361:200809767)
- Hernquist, L. 1990, *ApJ*, 356, 359, doi: [10.1086/168845](https://doi.org/10.1086/168845)
- Hills, J. G. 1988, *Nature*, 331, 687, doi: [10.1038/331687a0](https://doi.org/10.1038/331687a0)
- Huang, Y., Li, Q., Zhang, H., Li, X., & Sun, W. 2021, *ApJL*, 907, L42, doi: [10.3847/2041-8213/abd413](https://doi.org/10.3847/2041-8213/abd413)
- Johnson, D. R. H., & Soderblom, D. R. 1987, *AJ*, 93, 864, doi: [10.1086/114370](https://doi.org/10.1086/114370)
- Jurić, M., Ivezić, Ž., Brooks, A., Lupton, R. H., & Schlegel, D. 2008, *ApJ*, 673, 864, doi: [10.1086/523619](https://doi.org/10.1086/523619)
- Katz, D., Sartoretti, P., Guerrier, A., Panuzzo, P., & Seabroke, G. M. 2023, *A&A*, 674, A5, doi: [10.1051/0004-6361/202244220](https://doi.org/10.1051/0004-6361/202244220)

- Koposov, S. E., Boubert, D., Li, T. S., Erkal, D., & Da Costa, G. S. 2020, *MNRAS*, 491, 2465, doi: [10.1093/mnras/stz3081](https://doi.org/10.1093/mnras/stz3081)
- Li, H., Du, C., Ma, J., Shi, J., & Newberg, H. J. 2022, *ApJL*, 933, L13, doi: [10.3847/2041-8213/ac786d](https://doi.org/10.3847/2041-8213/ac786d)
- Li, Q.-Z., Huang, Y., Dong, X.-B., Zhang, H.-W., & Beers, T. C. 2023, *AJ*, 166, 12, doi: [10.3847/1538-3881/acd1dc](https://doi.org/10.3847/1538-3881/acd1dc)
- Li, T. S., Koposov, S. E., Zucker, D. B., Lewis, G. F., & Kuehn, K. 2019, *MNRAS*, 490, 3508, doi: [10.1093/mnras/stz2731](https://doi.org/10.1093/mnras/stz2731)
- Li, Y.-B., Luo, A. L., Lu, Y.-J., Zhang, X.-S., & Li, J. 2021, *ApJS*, 252, 3, doi: [10.3847/1538-4365/abc16e](https://doi.org/10.3847/1538-4365/abc16e)
- Liao, J., Du, C., Li, H., Ma, J., & Shi, J. 2023, *ApJL*, 944, L39, doi: [10.3847/2041-8213/acb7d9](https://doi.org/10.3847/2041-8213/acb7d9)
- Lindgren, L., Bastian, U., Biermann, M., Bombrun, A., & de Torres, A. 2021a, *A&A*, 649, A4, doi: [10.1051/0004-6361/202039653](https://doi.org/10.1051/0004-6361/202039653)
- Lindgren, L., Klioner, S. A., Hernández, J., Bombrun, A., & Ramos-Lerate, M. 2021b, *A&A*, 649, A2, doi: [10.1051/0004-6361/202039709](https://doi.org/10.1051/0004-6361/202039709)
- Majewski, S. R., Schiavon, R. P., Frinchaboy, P. M., Allende Prieto, C., & Barkhouser, R. 2017, *AJ*, 154, 94, doi: [10.3847/1538-3881/aa784d](https://doi.org/10.3847/1538-3881/aa784d)
- Marchetti, T. 2021, *MNRAS*, 503, 1374, doi: [10.1093/mnras/stab599](https://doi.org/10.1093/mnras/stab599)
- McConnachie, A. W. 2012, *AJ*, 144, 4, doi: [10.1088/0004-6256/144/1/4](https://doi.org/10.1088/0004-6256/144/1/4)
- McMillan, P. J. 2017, *MNRAS*, 465, 76, doi: [10.1093/mnras/stw2759](https://doi.org/10.1093/mnras/stw2759)
- Minniti, D., Fernández-Trincado, J. G., Smith, L. C., Lucas, P. W., & Gómez, M. 2021, *A&A*, 648, A86, doi: [10.1051/0004-6361/202039820](https://doi.org/10.1051/0004-6361/202039820)
- Miyamoto, M., & Nagai, R. 1975, *PASJ*, 27, 533
- Moni Bidin, C., Mauro, F., Geisler, D., Minniti, D., & Catelan, M. 2011, *A&A*, 535, A33, doi: [10.1051/0004-6361/201117488](https://doi.org/10.1051/0004-6361/201117488)
- Navarro, J. F., Frenk, C. S., & White, S. D. M. 1996, *ApJ*, 462, 563, doi: [10.1086/177173](https://doi.org/10.1086/177173)
- Paxton, B., Bildsten, L., Dotter, A., et al. 2011, *ApJS*, 192, 3, doi: [10.1088/0067-0049/192/1/3](https://doi.org/10.1088/0067-0049/192/1/3)
- Paxton, B., Cantiello, M., Arras, P., et al. 2013, *ApJS*, 208, 4, doi: [10.1088/0067-0049/208/1/4](https://doi.org/10.1088/0067-0049/208/1/4)
- Paxton, B., Marchant, P., Schwab, J., et al. 2015, *ApJS*, 220, 15, doi: [10.1088/0067-0049/220/1/15](https://doi.org/10.1088/0067-0049/220/1/15)
- Petts, J. A., Read, J. I., & Gualandris, A. 2016, *MNRAS*, 463, 858, doi: [10.1093/mnras/stw2011](https://doi.org/10.1093/mnras/stw2011)
- Portegies Zwart, S. F. 2000, *ApJ*, 544, 437, doi: [10.1086/317190](https://doi.org/10.1086/317190)
- Price-Whelan, A. M. 2017, *Journal of Open Source Software*, 2, 388, doi: [10.21105/joss.00388](https://doi.org/10.21105/joss.00388)
- Quispe-Huaynasi, F., Roig, F., McDonald, D. J., Loaiza-Tacuri, V., & Majewski, S. R. 2022, *AJ*, 164, 187, doi: [10.3847/1538-3881/ac90bc](https://doi.org/10.3847/1538-3881/ac90bc)
- Schönrich, R., Binney, J., & Dehnen, W. 2010, *MNRAS*, 403, 1829, doi: [10.1111/j.1365-2966.2010.16253.x](https://doi.org/10.1111/j.1365-2966.2010.16253.x)
- Shen, K. J., Boubert, D., Gänsicke, B. T., et al. 2018, *ApJ*, 865, 15, doi: [10.3847/1538-4357/aad55b](https://doi.org/10.3847/1538-4357/aad55b)
- Steinmetz, M., Guiglion, G., McMillan, P. J., Matijević, G., & Enke, H. 2020, *AJ*, 160, 83, doi: [10.3847/1538-3881/ab9ab8](https://doi.org/10.3847/1538-3881/ab9ab8)
- van der Marel, R. P., & Kallivayalil, N. 2014, *ApJ*, 781, 121, doi: [10.1088/0004-637X/781/2/121](https://doi.org/10.1088/0004-637X/781/2/121)
- Vasiliev, E. 2019, *MNRAS*, 484, 2832, doi: [10.1093/mnras/stz171](https://doi.org/10.1093/mnras/stz171)
- Vasiliev, E., & Baumgardt, H. 2021, *MNRAS*, 505, 5978, doi: [10.1093/mnras/stab1475](https://doi.org/10.1093/mnras/stab1475)
- Vasiliev, E., & Belokurov, V. 2020, *MNRAS*, 497, 4162, doi: [10.1093/mnras/staa2114](https://doi.org/10.1093/mnras/staa2114)
- Vasiliev, E., Belokurov, V., & Erkal, D. 2021, *MNRAS*, 501, 2279, doi: [10.1093/mnras/staa3673](https://doi.org/10.1093/mnras/staa3673)
- Wang, B., & Han, Z. 2009, *A&A*, 508, L27, doi: [10.1051/0004-6361/200913326](https://doi.org/10.1051/0004-6361/200913326)
- Wang, B., Justham, S., & Han, Z. 2013, *A&A*, 559, A94, doi: [10.1051/0004-6361/201322298](https://doi.org/10.1051/0004-6361/201322298)
- Weatherford, N. C., Kiroğlu, F., Fragione, G., Chatterjee, S., & Kremer, K. 2023, *ApJ*, 946, 104, doi: [10.3847/1538-4357/acbcc1](https://doi.org/10.3847/1538-4357/acbcc1)
- Yang, C., Xue, X.-X., Li, J., Liu, C., & Zhang, B. 2019, *ApJ*, 886, 154, doi: [10.3847/1538-4357/ab48e2](https://doi.org/10.3847/1538-4357/ab48e2)
- Zhao, G., Zhao, Y.-H., Chu, Y.-Q., Jing, Y.-P., & Deng, L.-C. 2012, *Research in Astronomy and Astrophysics*, 12, 723, doi: [10.1088/1674-4527/12/7/002](https://doi.org/10.1088/1674-4527/12/7/002)